Optical Fiber Technology 55 (2020) 102146

Contents lists available at ScienceDirect

Optical Fiber Technology

journal homepage: www.elsevier.com/locate/yofte

Fiber interferometer based on standard fiber spliced between two thin-core insertions

Oleg V. Ivanov[a,b,c,*]

[a] Ulyanovsk Branch of Kotel'nikov Institute of Radio Engineering and Electronics of Russian Academy of Sciences, Ulitsa Goncharova 48, Ulyanovsk 432071, Russia
[b] Ulyanovsk State University, Ulitsa L. Tolstogo 42, Ulyanovsk 432970, Russia
[c] Ulyanovsk State Technical University, Ulitsa Severny Venets 32, Ulyanovsk 432027, Russia

ARTICLE INFO

Keywords:
Fiber interferometer
Fiber sensor
Cladding mode

ABSTRACT

A new type of fiber interferometer based on two short thin-core fiber insertions with a section of standard fiber in between is proposed. The thin-core fiber insertions excite cladding modes and provide energy exchange between different fiber modes. We have simulated and measured transmission through a single thin-core fiber section. The standard fiber section is used to accumulate phase differences between core and cladding modes propagating through the structure. Transmission spectra are measured for various lengths of the interferometer. Separate control of thin-core and standard fiber insertions adds flexibility in obtaining spectra desirable for sensing applications.

1. Introduction

Fiber structures with various insertions of nonstandard fibers, gratings, and tapers that are used to excite cladding modes have attracted considerable interest in recent years due to their compactness, simplicity of fabrication, and good sensitivity to parameters of external medium [1–3]. These structures find application in fiber sensors of humidity [4], temperature [5], refractive index [6–9], and liquid level [10–12]. Insertions of multimode [7,13], thin-core [4,8–10,14–16], coreless [11,17,18], depressed cladding [19–21], and microstructured fibers [22] are spliced with the standard fiber to provide coupling from the core mode to cladding modes.

In order to enhance sensitivity of fiber structures employing cladding modes, interferometers are created by combining two elements that couple different fiber modes. For example, it can be two sections of multimode fiber [7,13], pair of tapers [12,14] or taper and grating [2,23], etc. For sensors working in reflection, an interferometer can be made using just one element that is passed by the modes twice [9–11,18]. A modal interferometer is formed by a section of thin-core (TC) fiber spliced between standard fibers [4,15,16,21,24]. In such a structure, the cladding modes are excited at the junction of two fibers due to strong dissimilarity of their refractive index profiles.

Although the interferometer based on a section of TC fiber is a good sensing element, it has a drawback of difficulty to control independently coupling strength between modes and the length of the interferometer. If narrow spectral peaks are desirable, the interferometer should be long, which may result in very small amplitude of the core mode and high losses in the transmission of the whole structure. So, separate control of coupling strength and interferometer length is needed.

In this paper, we propose a new type of fiber interferometer based on two short TC fiber insertions separated by a section of standard fiber. The coupling strength between modes can be tuned to optimal value by changing the length of the insertions, while the phase difference is determined by the length of the standard fiber between the TC insertions. We study the dependence of transmission spectrum on the length of the TC fiber insertions in experiment and compare with simulation. We measure the spectrum for different lengths of the standard fiber and describe how it depends on parameters of the structure.

2. Fiber structure

The interferometer fiber structure is formed by two sections of TC fiber spliced by a conventional fusion splicer. As a section of TC fiber, we used SM600 from Fibercore. Standard SMF-28 fiber from Corning is placed between the two TC insertions and works as a base of interferometer (Fig. 1). Its length can vary from 1 to 30 cm.

The TC fiber is cleaved to obtain sections of length of about 1 mm and shorter. Since such fiber length cannot be produced directly by standard cleaver, we employ the following procedure: SMF-28 is

* Address: Ulyanovsk Branch of Kotel'nikov Institute of Radio Engineering and Electronics of Russian Academy of Sciences, Ulitsa Goncharova 48, Ulyanovsk 432071, Russia.
E-mail address: olegivvit@yandex.ru.

https://doi.org/10.1016/j.yofte.2020.102146
Received 25 October 2019; Accepted 9 January 2020
Available online 18 January 2020
1068-5200/

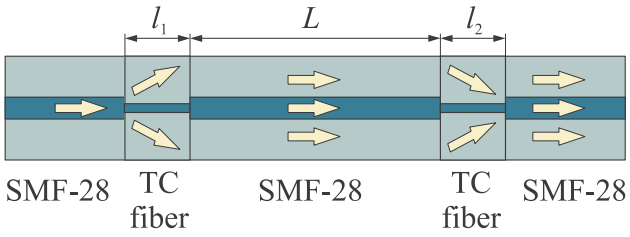

Fig. 1. Structure of fiber interferometer with two TC insertions and scheme of light propagation.

cleaved in a fixed position in the cleaver. Cleaved ends of SMF-28 and SM600 are spliced. SMF-28 fiber with SM600 at its tip is placed in the cleaver in the same position as before splicing and is shifted by the required length of the TC section, so that the blade is under SM600. SM600 is cut in this shifted point, and a short section of it is left at the end of SMF-28. Then, this fiber structure is spliced with another SMF-28 fiber.

Light from a broadband source is launched into the structure from SMF-28 fiber, passes the interferometer, and is transmitted through the same type of fiber to an optical spectrum analyzer. SM600 fiber of the TC insertion is designed for single-mode operation at wavelengths 630–780 nm; therefore, this fiber has a small core: $r_{co} \sim 2.2$ μm (NA = 0.12, $\lambda_{cutoff} \sim 550$ nm). Its cladding has standard radius $r_{cl} = 62.5$ μm. The polymer jackets of the TC fiber insertions and SMF-28 fiber of the interferometer base are removed to avoid losses of cladding modes due to coupling into the jacket.

3. Experimental spectra

For obtaining maximum modulation amplitude in the transmission spectrum, two interfering modes should have equal amplitudes. Therefore, we need to prepare such an insertion of TC fiber at one side of the interferometer that the power of one cladding mode is equal to the power remaining in the core mode. Besides, some power is distributed between unwanted cladding modes. Thus, the optimum power in the core mode after single insertion of TC fiber should be 30–50%.

If the fiber core is not quite thin compared to the standard fiber, then the mode profiles of the spliced fibers are similar and coupling to the cladding modes is not strong enough. We experimented with several different TC fibers from Fibercore: SM800, SM750, and SM600. We found that a 3-mm insertion of SM800 fiber with 5.6-μm core couples less than 20% of core mode power to cladding modes. An insertion made of SM750 fiber couples up to 40% to cladding modes. In cases of these fibers, it is not possible to enhance coupling to cladding modes by increasing the length of the insertion. SM600 fiber has a core thin enough to convert more than 50% of core mode, and it is suitable for our interferometer.

On the other hand, it is desirable to excite modes with amplitudes that almost independent of wavelength. Therefore, we studied the wavelength dependence of transmission on the insertion length of SM600 fiber. The results of measurements are demonstrated in Fig. 2.

The length of TC fiber was changed from 2 mm to 0.1 mm by consecutive cleaving and subsequent splicing with the standard fiber. When insertion length increases from 0.1 to 1.5 mm, transmission goes down demonstrating some descent of curves at longer wavelength. For length longer than 1.5 mm, transmission discontinues smooth decreasing and becomes a nonmonotonic function of insertion length and wavelength, because an interferometer is formed by the TC insertion between two splices [1,8]. For the purpose of creating one side of interferometer, the optimum length of TC insertion made of SM600 fiber is 0.3–0.8 mm.

Using a fusion splicing machine, we created an interferometer with two TC insertions of SM600 fiber having lengths 0.3 and 0.5 mm. The initial length of SMF-28 fiber between TC insertions was 194 mm. Then,

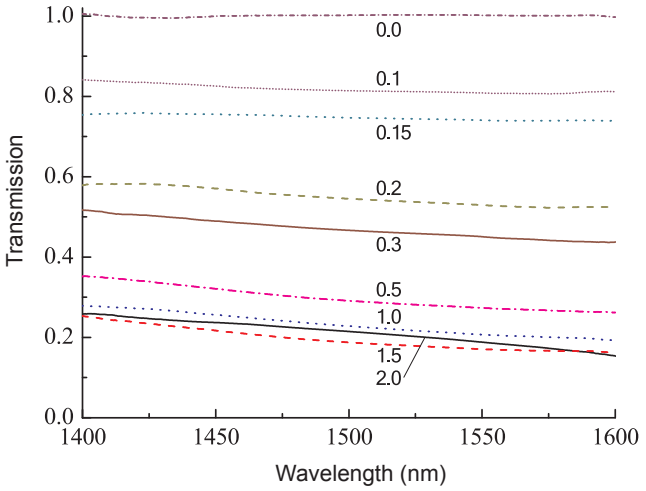

Fig. 2. Transmission of a single TC insertion for various lengths of SM600 fiber (indicated in mm).

SMF-28 fiber was cleaved in the middle and shortened by several centimeters. This procedure was repeated nine times. Each time transmission spectrum was measured. The final length was 21 mm. The resulting transmission spectra of the interferometer for some lengths of the base SMF-28 fiber are shown in Fig. 3. The spectrum curve oscillates between 0.05 and 0.40. The period of oscillations in wavelength is inversely proportional to the length of the interferometer. So, the period is about 2.8 nm for $L = 194$ mm and 21 nm for $L = 21$ mm.

The dependence of the number of peaks in the transmission spectrum of TC fiber structure as a function of interferometer length is demonstrated in Fig. 4. We can see that the dependence is quite linear

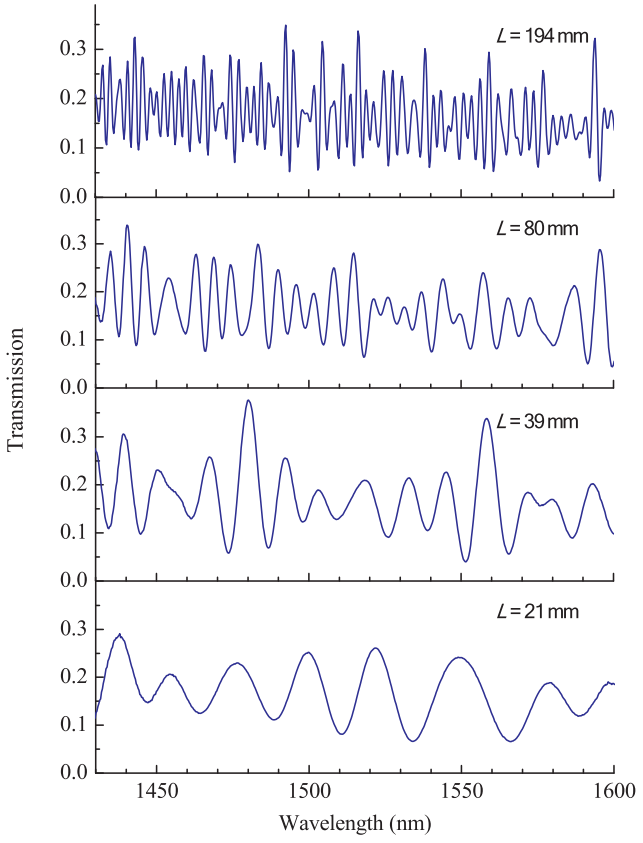

Fig. 3. Transmission spectra of TC fiber structure for different lengths of the interferometer.

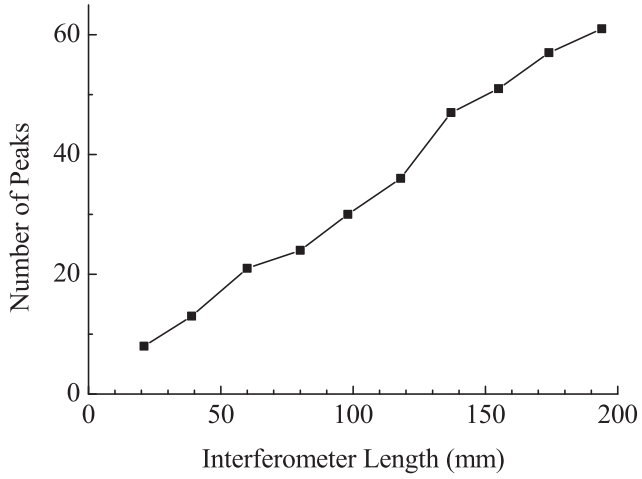

Fig. 4. Number of peaks in transmission spectrum of TC fiber structure as a function of interferometer length.

and the number of peaks is proportional to the interferometer length, which is in accordance with the relation describing the wavelength spacing of interference spectrum in the case of two-mode interference:

$$\Delta\lambda = \frac{\lambda^2/L}{dn_2/d\lambda - dn_1/d\lambda - \lambda(n_2 - n_1)} \quad (1)$$

where n_1 and n_2 are the effective refractive indices of two interfering fiber modes.

In reality, there are more than two interfering modes; therefore, the transmission curve is not a perfect sinusoidal function, but it has irregular phase and amplitude changes. From Fig. 3, we can also notice that the oscillation period changes with wavelength. To analyze the dependence of this period on wavelength, we depicted in Fig. 5 a spectrogram of the transmission spectrum of TC interferometer with 194-cm section of standard fiber. As can be seen, the frequency decreases with wavelength, and the period increases, which agrees with Eq. (1). Irregularity of oscillations results in a tangled spectrogram, indicating that it is produced by multimode interference.

4. Simulation

In experiment, we are not able to change continuously the length of the TC fiber with a small step, because it is difficult to perform accurate cleaving at a distance less than 0.2 mm from previous splicing point. Therefore, we obtain the dependence of transmission through a single TC fiber section on its length by simulation. We use the following parameters of the TC fiber (SM600): r_{co} = 2.2 μm, Δn_{co} = 0.0034. The TC fiber section is placed between SMF-28 fibers having core radius r_{co} = 4.2 μm and Δn_{co} = 0.0054. The cladding radius is 62.5 μm for both the fibers.

When light is launched into the interferometer, the core mode of the standard fiber is coupled at the first splicing point to the core and cladding modes of SM600 fiber. The power coupled to each mode can be calculated as an overlap integral over the fiber cross section between profiles of the field of the input mode of SMF-28 and the fields of modes of the TC fiber. High order cladding modes have small overlap integrals with the input core mode and get less power than low order modes; therefore, we can neglect modes of very high orders. In our simulation, we take into account first 50 modes of SM600 fiber.

The core and cladding modes propagate with different propagation constants through the section of SM600 fiber. The modes come to the second splicing point with different phases. At this point, the modes of SM600 fiber are coupled to the core mode of the standard fiber. The power coupled from each mode of SM600 fiber to the core mode of SMF-28 fiber is determined by the same overlap integrals. The resulting mode is an interference field of all the modes, which can be found by summation of mode amplitudes with account of the phases accumulated during propagation through the length of SM600 fiber.

The results of simulation of transmission through a single TC fiber section for tree wavelengths as a function of its length are shown in Fig. 6. It is seen that transmission decreases monotonically with length increasing up to 1.2 mm. Transmission is lower for longer wavelength. We can observe such behavior in experiment (Fig. 2). For lengths of the fiber section larger than 1.2 mm, monotonic curves begin to oscillate with increasing amplitudes. These oscillations are related to multimode interference appearing, when the core mode and low order cladding modes accumulate phase difference of about π. In addition, the dependence of transmission on wavelength becomes stronger in this case. At longer wavelength, the loss is higher for all lengths and the transmission curve goes down, as we can also see in Fig. 2. The experimental dots lie somewhat below the simulation curves, which is probably caused by imperfect splicing of the two fibers. Precise cleaving and splicing with accuracy of about 0.1 mm is needed for observing oscillations on the TC section length.

So, simulation confirms that if one wants to create an interferometer using a couple of TC fiber sections based on SM600, it is preferable to use sections of length below 1.0 mm in order to avoid additional

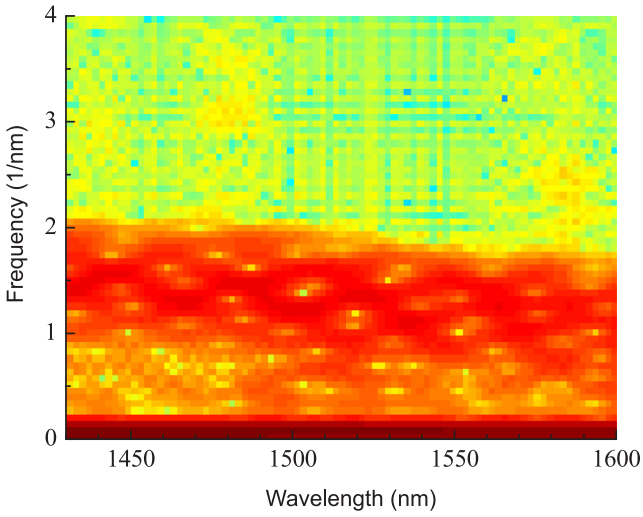

Fig. 5. Spectrogram of transmission spectrum of TC fiber structure with a 194-cm base.

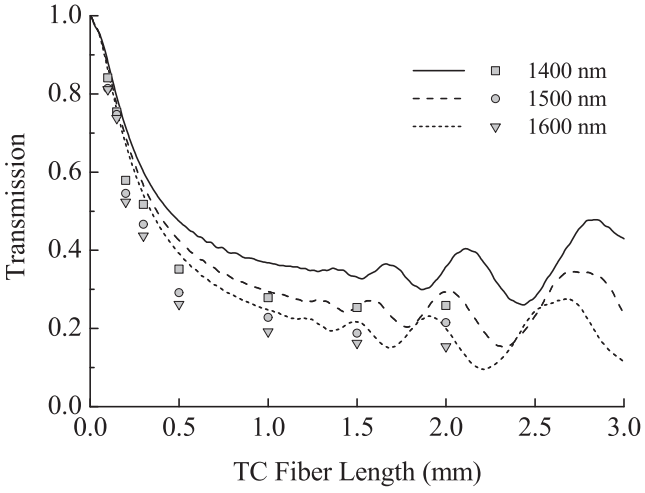

Fig. 6. Transmission through a single TC fiber section (SM600) for several wavelengths as a function of its length: simulation (curves) and experiment (dots).

interference in the TC section itself. On the other hand, the length should not be too small (less than 0.2 mm), otherwise coupling strength to cladding modes would be insufficient.

The interferometer proposed in this work can be used in various sensing applications, for example, as a sensor of bending or refractive index. The TC interferometer should be sensitive to the external refractive index due to the fact that the cladding modes guided by the outer surface of the cladding of SM630 fiber have their evanescent field propagating through the external medium. The interference fringes serving for observation of wavelength shifts can be made quite narrow and sensitive to phase changes of the core and cladding modes that are induced by changing various physical parameters.

5. Conclusion

We have presented a new type of fiber interferometer based on two short thin-core fiber insertions with a section of standard fiber between them. The thin-core fiber insertions excite cladding modes and provide energy exchange between different fiber modes. The coupling strength and phase difference between modes are determined by the lengths of the insertions and the standard fiber, respectively. Separate control of these parameters adds flexibility in obtaining spectra desirable for sensing applications. We have simulated and measured transmission through a single thin-core fiber section. The optimum length of this section is 0.3–0.8 mm. Transmission spectra of the interferometer demonstrating oscillating behavior are measured for its various lengths. The period of oscillations in the spectrum is inversely proportional to the interferometer length and increases with wavelength.

Acknowledgment

This work was carried out within the framework of the state task.

References

[1] Hidayah S. Nur, A.R. Hanim, H. Hazura, A.S.M. Zain, S.K. Idris, Modal interferometer structures and splicing techniques of fiber optic sensor, J. Telecomm. Electron. Comp. Eng. 10 (2018) 23–27.
[2] C. Tong, X. Chen, Y. Zhou, et al., Ultra-long-period fiber grating cascaded to a knob-taper for simultaneous measurement of strain and temperature, Opt. Rev. 25 (2018) 295–300.
[3] O.V. Ivanov, Mode interaction in a structure based on optical fiber with depressed inner cladding, J. Comm. Tech. Electron. 63 (2018) 1143–1151.
[4] S. Akita, H. Sasaki, K. Watanabe, A. Seki, A humidity sensor based on a hetero-core optical fiber, Sens. Act. B: Chem. 147 (2010) 385–391.
[5] W. Bao, N. Hu, X. Qiao, et al., High-temperature properties of a thin-core fiber MZI with an induced refractive index modification, IEEE Photonics Technol. Lett. 28 (2016) 2245–2248.
[6] Y. Zhao, F. Pang, Y. Dong, et al., Refractive index sensitivity enhancement of optical fiber cladding mode by depositing nanofilm via ALD technology, Opt. Express 21 (2013) 26136–26143.
[7] X. Dong, H. Du, Zh. Luo, K. Yin, J. Duan, Highly sensitive refractive index sensor based on novel Mach-Zehnder interferometer with multimode fiber–thin core fiber–multimode fiber structure, Jap. J. Appl. Phys. 57 (2018) 092501.
[8] B. Xu, I.J.-Q. Li, Y. Li, X.-Y. Dong, A thin-core fiber modal interferometer for liquid-level sensing, Chin. Phys. Lett. 29 (2012) 104209.
[9] X. Ben, L. Yi, D. Xin-Yong, J. Shang-Zhong, Z.H. Zai-Xuan, Highly sensitive refractive index sensor based on a cladding-etched thin-core fiber sandwiched between two single-mode fibers, Chin. Phys. Lett. 29 (2012) 094203.
[10] B. Gu, W. Qi, Y. Zhou, et al., Reflective liquid level sensor based on modes conversion in thin-core fiber incorporating tilted fiber Bragg grating, Opt. Express 22 (2014) 11834–11839.
[11] J.E. Antonio-Lopez, J.J. Sanchez-Mondragon, P. LiKamWa, D.A. May-Arrioja, Fiber-optic sensor for liquid level measurement, Opt. Lett. 36 (2011) 3425–3427.
[12] X. Wen, T. Ning, C. Li, et al., Liquid level measurement by applying the Mach-Zehnder interferometer based on up-tapers, Appl. Opt. 53 (2014) 71–75.
[13] J. Su, Zh. Tong, Y. Cao, W. Zhang, High sensitivity multi-mode–multimode–multimode structure fiber sensor based on modal interference, Opt. Commun. 315 (2014) 112–115.
[14] Zh. Tong, X. Wang, W. Zhang, L. Xue, Research on dual-parameter optical fiber sensor based on thin-core fiber and spherical structure, Laser Phys. 28 (2018) 045102.
[15] X. Huang, X. Li, J. Yang, C. Tao, X. Guo, H. Bao, Y. Yin, H. Chen, Y. Zhu, An in-line Mach-Zehnder interferometer using thin-core fiber for ammonia gas sensing with high sensitivity, Sci. Rep. 7 (2017) 44994.
[16] M. Engholm, H. Krister, H. Andersson, M. Sandberg, H.-E. Nilsson, A bio-compatible fiber optic pH sensor based on a thin core interferometric technique, Photonics 6 (2019) 11.
[17] J.-X. Shao, W.-G. Xie, X. Song, Y.-N. Zhang, A new hydrogen sensor based on SNS fiber interferometer with Pd/WO3 coating, Sensors 17 (2017) 2144.
[18] S. Novais, M.S. Ferreira, J.L. Pinto, Relative humidity fiber sensor based on multimode interferometer coated with agarose-gel, Coatings 8 (2018) 453.
[19] X. Fu, H. Xie, C. Zhang, P. Guo, G. Fu, W. Bi, Fiber-optic temperature sensor based on specialty triple-clad fiber, Proc. SPIE 9274, Adv. Sensor Syst. Appl. VI (2014) 92741P.
[20] O.V. Ivanov, I.V. Zlodeev, Fiber structure based on depressed inner cladding fiber for bend, refractive index and temperature sensing, Meas. Sci. Technol. 25 (2014) 015201.
[21] Y. Zhao, F. Pang, Y. Dong, J. Wen, Z. Chen, T. Wang, Refractive index sensitivity enhancement of optical fiber cladding mode by depositing nanofilm via ALD technology, Opt. Express 21 (2013) 26136–121143.
[22] T. Li, X. Donga, C.C. Chanb, L. Hua, W. Qian, Simultaneous strain and temperature measurement based on a photonic crystal fiber modal-interference interacting with a long period fiber grating, Opt. Commun. 285 (2012) 4874–4877.
[23] X. Dong, L. Su, P. Shum, Y. Chung, Wavelength-selective all-fiber filter based on a single long-period fiber grating and a misaligned splicing point, Opt. Commun. 258 (2006) 159–163.
[24] O.V. Ivanov, F. Yang, F. Tian, H. Du, Thin-core fiber structures with overlays for sensing applications, Opt. Express 25 (2017) 31197–31203.